

Reconsideration of Nonequilibrium Perturbative Formalism and Spectral Function for the Anderson Model

Mami Hamasaki

Department of Physics, Kyoto University, Kyoto 606-8502, Japan

February 20, 2019

The nonequilibrium perturbative formalism is reconsidered and the improvement of the relations for self-energy is introduced into the formalism. As the consequence, it is found that some equations formally used are not exact and proves that the nonequilibrium (real-time) perturbative expansion can be connected with the Matsubara imaginary-time perturbative expansion for equilibrium. Then, it is confirmed that by the improvement, the nonequilibrium perturbative equation in matrix form works as the Dyson's equation at least up to the fourth-order. Additionally, as the numerical results, the Kondo resonance disappears for bias voltage exceeding the Kondo temperature; it has been observed experimentally.

Key words: nonequilibrium perturbative formalism, nonequilibrium Green's function, Kondo effect, Dyson's equation

PACS: 71.15.-m, 05.70.Ln

1. Introduction

1.1. Nonequilibrium Perturbative Formalism

The basic idea on the nonequilibrium perturbation theory grounded on the time-contour which starts and ends at $t = -\infty$ via $t = \infty$ has been proposed by Schwinger. [1]

After that, the frame of the nonequilibrium perturbation theory has been built up using the nonequilibrium Green's functions given after the time-contour by Keldysh. [2] The perturbative equation is expressed in matrix form:

$$\mathbf{G} = \mathbf{g} + \mathbf{g} \mathbf{\Sigma} \mathbf{G}, \quad (1)$$

where

$$\mathbf{G} = \begin{bmatrix} G^{--} & G^{<} \\ G^{>} & G^{++} \end{bmatrix}, \quad \mathbf{\Sigma} = \begin{bmatrix} \Sigma^{--} & \Sigma^{<} \\ \Sigma^{>} & \Sigma^{++} \end{bmatrix}.$$

The nonequilibrium Green's functions are given in the Heisenberg representation by

$$G^{--}(t_1, t_2) \equiv -i \langle T \hat{d}(t_1) \hat{d}^\dagger(t_2) \rangle, \quad (2)$$

$$G^{++}(t_1, t_2) \equiv -i \langle \tilde{T} \hat{d}(t_1) \hat{d}^\dagger(t_2) \rangle, \quad (3)$$

$$G^{>}(t_1, t_2) \equiv -i \langle \hat{d}(t_1) \hat{d}^\dagger(t_2) \rangle, \quad (4)$$

$$G^{<}(t_1, t_2) \equiv i \langle \hat{d}^\dagger(t_2) \hat{d}(t_1) \rangle. \quad (5)$$

Here, the time ordering operator T arranges in chronological order and \tilde{T} is the anti time ordering operator which arranges in the reverse of chronological order. The angular brackets denote thermal average in nonequilibrium.

Can Equation (1) be the Dyson's equation exactly? Some researchers insist that the equation is the exact Dyson's equation, while some say that Equation (1) should not be used excepting the lowest-order perturbation like the first-order of transfer. Thus I try to confirm this point in this work.

1.2. The Kondo effect

The Kondo effect [3] was discovered forty years ago and after that, the Kondo physics has been clarified from Landau's Fermi liquid theory [4], the renormalization group [5], scaling [6], etc.. Besides, generalized Kondo problem, that of more than one channel or one impurity has been investigated. [7, 8] Then, the Kondo effect in electron transport through a quantum dot has been predicted theoretically at the end of 1980s [9] and after a decade, this phenomenon has been observed. [10] The Kondo effect has been studied theoretically using the Anderson model and the predictions have been confirmed experimentally. In the Kondo regime, the conductance has been observed to reach the unitarity limit and the Kondo temperature estimated from observation [11] is in excellent agreement with the expression derived using the Anderson model. [12] Furthermore, the Kondo effect in a quantum dot has been studied for nonequilibrium system where the bias voltage is applied. [13] The Yamada-Yosida theory, [14] perturbation theory for equilibrium based on the Fermi liquid theory [4] has been extended to nonequilibrium system and it has been shown that for bias voltage higher than the Kondo temperature, the Kondo resonance disappears in the spectral function with the second-order self-energy for the Anderson model. [15] In experiment, it has been observed that the Kondo effect is suppressed when source-drain bias voltage is comparable to or exceeds the Kondo temperature. [16, 17]

In the present work, the self-energy higher than the second-order has been formulated and the behavior of Kondo resonance has been investigated for nonequilibrium state.

2. Nonequilibrium Perturbation Theory

2.1. Formalism

A thermal average can be obtained on the basis of the nonequilibrium perturbation theory. [1, 2, 18, 19, 20, 21, 22] When the time evolution of the state is irreversible, then, the state at $t = \infty$ cannot be well-defined. One can know only the state at $t = -\infty$. Therefore, the time evolution is performed along the real-time contour which starts and ends at $t = -\infty$, as illustrated in Fig. 1.

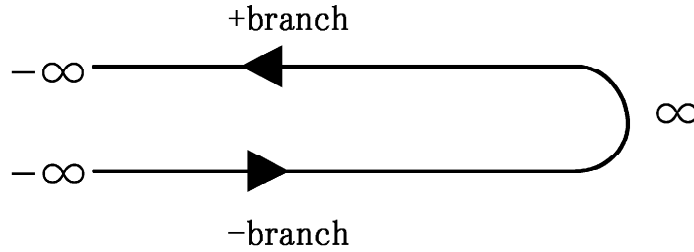


Figure 1. The time-contour which starts and ends at $t = -\infty$.

S matrix is defined by

$$\begin{aligned} \mathcal{S}(t, t_0) &= 1 + \sum_{n=1}^{\infty} \frac{1}{n!} \left(\frac{-i}{\hbar} \right)^n \int_{t_0}^t dt_1 \dots \int_{t_0}^t dt_n \mathcal{T} \left[\tilde{\mathcal{H}}_I(t_1) \dots \tilde{\mathcal{H}}_I(t_n) \right] \\ &= \mathcal{T} \left[\exp \left\{ \frac{-i}{\hbar} \int_{t_0}^t dt' \tilde{\mathcal{H}}_I(t') \right\} \right], \end{aligned} \quad (6)$$

$$\mathcal{S}(t, t_0)^\dagger = \mathcal{S}(t_0, t) = \tilde{\mathcal{T}} \left[\exp \left\{ \frac{i}{\hbar} \int_{t_0}^t dt' \tilde{\mathcal{H}}_I(t') \right\} \right]. \quad (7)$$

Here $\tilde{\mathcal{H}}_I$ is perturbation term in interaction representation.

For thermal equilibrium, the statistical operator (density matrix) is written in Gibbs form for the grand canonical ensemble by

$$\varrho_G = \frac{e^{-\beta(\mathcal{H}-\mu N)}}{\text{Tre}^{-\beta(\mathcal{H}-\mu N)}} = e^{\beta(\Omega-\mathcal{H}+\mu N)}. \quad (8)$$

However, Equation (8) is not valid exactly for nonequilibrium. We have no specific limitations upon the statistical operator. The statistical operator can generally be expressed in Schrödinger representation by [20, 22]

$$\varrho_S(t) = \sum_m |m_S(t) \rangle P_m \langle m_S(t)|. \quad (9)$$

Here, P_m is probability that the system is in state m and $|m_S(t) \rangle$ is the state in Schrödinger representation. ϱ_S satisfies the Liouville equation by

$$i\hbar \frac{\partial \varrho_S}{\partial t} = [\mathcal{H}, \varrho_S]. \quad (10)$$

The statistical operator in the interaction representation is given by $\tilde{\varrho}(t) = e^{i\mathcal{H}_0 t/\hbar} \varrho_S(t) e^{-i\mathcal{H}_0 t/\hbar}$ and satisfies

$$i\hbar \frac{\partial \tilde{\varrho}}{\partial t} = [\tilde{\mathcal{H}}_I, \tilde{\varrho}]. \quad (11)$$

As a matter of course, $\varrho_S(0) = \varrho(0) = \tilde{\varrho}(0)$. Here $\varrho(t)$ is in the Heisenberg representation. The time evolution is expressed using S matrix by

$$\tilde{\varrho}(t) = S(t, t_0) \tilde{\varrho}(t_0) S(t_0, t). \quad (12)$$

The thermal average in the Heisenberg representation at $t = 0$ can be obtained, for example by [22]

$$\begin{aligned} & \langle TA(t)B(t') \rangle \\ &= \text{Tr}[\varrho(0)TA(t)B(t')] \\ &= \text{Tr}[\tilde{\varrho}(-\infty)\mathcal{S}(-\infty, 0)TA(t)B(t')\mathcal{S}(0, -\infty)] \\ &= \text{Tr}[\tilde{\varrho}(-\infty)\mathcal{S}(-\infty, \infty)\{\mathcal{TS}(\infty, -\infty)\tilde{A}(t^-)\tilde{B}(t'^-)\}] \\ &= \sum_{n=1}^{\infty} \sum_{m=1}^{\infty} \frac{1}{n!} \frac{1}{m!} \left(\frac{i}{\hbar}\right)^n \left(\frac{-i}{\hbar}\right)^m \int_{-\infty}^{\infty} dt_1 \dots \int_{-\infty}^{\infty} dt_n \int_{-\infty}^{\infty} dt'_1 \dots \int_{-\infty}^{\infty} dt'_m \\ & \quad \times \langle \{ \tilde{\mathcal{T}}\tilde{\mathcal{H}}_I(t_1^+) \dots \tilde{\mathcal{H}}_I(t_n^+) \} \{ \mathcal{T}\tilde{\mathcal{H}}_I(t_1^-) \dots \tilde{\mathcal{H}}_I(t_m^-) \tilde{A}(t^-) \tilde{B}(t'^-) \} \rangle_{av}, \end{aligned}$$

where $\langle \dots \rangle_{av} = \text{Tr}[\tilde{\varrho}(-\infty) \dots]$.

2.2. Improvement for Relation of Self-Energy

After the perturbative expansion is executed, the retarded and advanced self-energies are formulated.

According to the definition, the retarded and advanced Green's functions are given by

$$G^r(t_1, t_2) \equiv -i\theta(t_1 - t_2) \langle \{ \hat{d}(t_1), \hat{d}^\dagger(t_2) \} \rangle, \quad (13)$$

$$G^a(t_1, t_2) \equiv i\theta(t_2 - t_1) \langle \{ \hat{d}(t_1), \hat{d}^\dagger(t_2) \} \rangle. \quad (14)$$

Here, the curly brackets denote anticommutator. The Dyson's equations are given by

$$G^r = g^r + g^r \Sigma^r G^r, \quad (15)$$

$$G^a = g^a + g^a \Sigma^a G^a. \quad (16)$$

If

$$\mathbf{L} = [\mathbf{L}^\dagger]^{-1} = \frac{1}{\sqrt{2}} \begin{bmatrix} 1 & -1 \\ 1 & 1 \end{bmatrix},$$

then,

$$\Sigma = \begin{bmatrix} \Sigma^{--} & \Sigma^< \\ \Sigma^> & \Sigma^{++} \end{bmatrix} \longrightarrow \mathbf{L}\Sigma\mathbf{L}^\dagger = \begin{bmatrix} \Omega & \Sigma^r \\ \Sigma^a & 0 \end{bmatrix}.$$

The relationship for self-energy is obtained by comparison of Eq. (1) with Eqs. (15) and (16). In this point, since Equation (1) is expressed independently of the definition of the Green's functions, it is required to improve as follows:

$$\Sigma^r(t) = [\Sigma^{--}(t) + \Sigma^<(t)]\theta(t) = -[\Sigma^{++}(t) + \Sigma^>(t)]\theta(t), \quad (17)$$

$$\Sigma^a(t) = [\Sigma^{--}(t) + \Sigma^>(t)]\theta(-t) = -[\Sigma^{++}(t) + \Sigma^<(t)]\theta(-t). \quad (18)$$

In general,

$$\begin{aligned} \Sigma^{--}(t) &\neq \Sigma^{--}(-t), & \Sigma^{++}(t) &\neq \Sigma^{++}(-t), \\ \Sigma^<(t) &\neq \Sigma^<(-t), & \Sigma^>(t) &\neq \Sigma^>(-t), \end{aligned}$$

because these self-energies include the Green's functions which change in dependence upon time:

$$\begin{aligned} g^{--}(t) &= \theta(t)g^>(t) + \theta(-t)g^<(t), & g^{++}(t) &= \theta(t)g^<(t) + \theta(-t)g^>(t), \\ g^r(t) &= \theta(t)[g^>(t) - g^<(t)], & g^a(t) &= \theta(-t)[g^<(t) - g^>(t)]. \end{aligned}$$

Although the step functions $\theta(t)$ and $\theta(-t)$ in Eqs. (17) and (18) are usually missing in the nonequilibrium perturbative formalism, they cannot be disregarded, especially in the high-order perturbation theory including multiple times.

Then, it proves that the relation formally used,

$$\Sigma^r(E) - \Sigma^a(E) = \Sigma^<(E) - \Sigma^>(E), \quad (19)$$

does not stand, though it may hold approximately in some simple cases. Additionally, since the relations,

$$\Sigma^r(t) = [\Sigma^{--}(t) + \Sigma^<(t)] = -[\Sigma^{++}(t) + \Sigma^>(t)], \quad (20)$$

$$\Sigma^a(t) = [\Sigma^{--}(t) + \Sigma^>(t)] = -[\Sigma^{++}(t) + \Sigma^<(t)]. \quad (21)$$

are not exact without the step functions, the equations derived from those relations

$$G^< = (1 + G^r \Sigma^r)g^<(1 + G^a \Sigma^a) - G^r \Sigma^< G^a, \quad (22)$$

$$G^> = (1 + G^r \Sigma^r)g^>(1 + G^a \Sigma^a) - G^r \Sigma^> G^a, \quad (23)$$

do not hold.

3. Expressions of Self-Energy for Anderson model

3.1. Anderson Model

We consider nonequilibrium stationary state. The system is described by the Anderson model connected to leads. The impurity with on-site energy E_0 and the Coulomb interaction U is connected to the left and right leads by the mixing matrix elements, v_L and v_R . The Anderson Hamiltonian is given by

$$\begin{aligned} \mathcal{H} = & E_0 \sum_{\sigma} \hat{n}_{d\sigma} + \mu_L \sum_{\sigma} \hat{n}_{L\sigma} + \mu_R \sum_{\sigma} \hat{n}_{R\sigma} + U(\hat{n}_{d\uparrow} - \langle \hat{n}_{d\uparrow} \rangle)(\hat{n}_{d\downarrow} - \langle \hat{n}_{d\downarrow} \rangle) \\ & - \sum_{\sigma} v_L (\hat{d}_{\sigma}^{\dagger} \hat{c}_{L\sigma} + \text{H.c.}) - \sum_{\sigma} v_R (\hat{d}_{\sigma}^{\dagger} \hat{c}_{R\sigma} + \text{H.c.}). \end{aligned} \quad (24)$$

\hat{d}^\dagger (\hat{d}) is creation (annihilation) operator for electron on the impurity, and \hat{c}_L^\dagger and \hat{c}_R^\dagger (\hat{c}_L and \hat{c}_R) are creation (annihilation) operators in the left and right leads, respectively. σ is index for spin. The chemical potentials in the isolated left and right leads are μ_L and μ_R , respectively. The applied voltage is, therefore defined by $eV \equiv \mu_L - \mu_R$.

We consider that the band-width of left and right leads is large infinitely, so that the coupling functions, Γ_L and Γ_R can be taken to be independent of energy, E . On-site energy E_0 is set canceling with the Hartree term, *i.e.* the first-order contribution to self-energy for electron correlation: $\Sigma_\sigma^{r(1)}(E) = \Sigma_\sigma^{a(1)}(E) = U\langle n_{-\sigma} \rangle$. Accordingly, the Fourier components of the noninteracting (unperturbed) Green's functions reduce to

$$g^r(E) = \frac{1}{E + i\Gamma}, \quad (25)$$

$$g^a(E) = \frac{1}{E - i\Gamma}, \quad (26)$$

where $\Gamma = (\Gamma_L + \Gamma_R)/2$. Hence, the inverse Fourier components can be written by

$$\begin{aligned} g^r(t) &= -i\theta(t)e^{-\Gamma t}, \\ g^a(t) &= i\theta(-t)e^{\Gamma t}. \end{aligned}$$

In addition,

$$g^<(E) = g^r(E) [if_L(E)\Gamma_L + if_R(E)\Gamma_R] g^a(E), \quad (27)$$

$$g^>(E) = g^r(E) [i(1 - f_L(E))\Gamma_L + i(1 - f_R(E))\Gamma_R] g^a(E). \quad (28)$$

f_L and f_R are the Fermi distribution functions in the isolated left and right leads, respectively. By Eqs. (27) and (28), the nonequilibrium state is introduced as the superposition of the left and right leads. Then, the effective Fermi distribution function can be expressed by [15]

$$f_{\text{eff}}(E) = \frac{f_L(E)\Gamma_L + f_R(E)\Gamma_R}{\Gamma_L + \Gamma_R}. \quad (29)$$

3.2. Self-Energy

The retarded and advanced self-energies cannot be written in energy representation; as a consequence, these are expressed as the Fourier transformation of time representation. The second-order self-energy is written by

$$\begin{aligned} \Sigma^{r(2)}(E) &= U^2 \int_0^\infty dt_1 e^{iEt_1} \begin{bmatrix} g^>(t_1)g^>(t_1)g^<(-t_1) \\ -g^<(t_1)g^<(t_1)g^>(-t_1) \end{bmatrix} \\ &= U^2 \int_0^\infty dt_1 e^{iEt_1} \begin{bmatrix} g^\pm(t_1)g^>(t_1)g^<(-t_1) \\ +g^<(t_1)g^\pm(t_1)g^>(-t_1) \\ +g^<(t_1)g^>(t_1)g^\pm(-t_1) \end{bmatrix}, \end{aligned} \quad (30)$$

$$\begin{aligned} \Sigma^{a(2)}(E) &= U^2 \int_{-\infty}^0 dt_1 e^{iEt_1} \begin{bmatrix} g^<(t_1)g^<(t_1)g^>(-t_1) \\ -g^>(t_1)g^>(t_1)g^<(-t_1) \end{bmatrix} \\ &= U^2 \int_{-\infty}^0 dt_1 e^{iEt_1} \begin{bmatrix} g^\pm(t_1)g^>(t_1)g^<(-t_1) \\ +g^<(t_1)g^\pm(t_1)g^>(-t_1) \\ +g^<(t_1)g^>(t_1)g^\pm(-t_1) \end{bmatrix}. \end{aligned} \quad (31)$$

Here $g^\pm(t) = g^r(t) + g^a(t)$, that is, $g^+(t) = g^r(t) = -i\theta(t)e^{-\Gamma t}$ for $t \geq 0$ and $g^-(t) = g^a(t) = i\theta(-t)e^{\Gamma t}$ for $t < 0$. Additionally, $g^<(t)$ and $g^>(t)$ are the inverse Fourier components of Eqs. (27) and (28). Figure 2 shows the diagram for the second-order self-energy. As shown numerically

later, the second-order contribution coincide with those derived by Hershfield *et al.* [15]. In the symmetric equilibrium case, the asymptotic behavior at low energy is expressed by

$$\Sigma^{r(2)}(E) \simeq -\Gamma \left(3 - \frac{\pi^2}{4}\right) \left(\frac{U}{\pi\Gamma}\right)^2 \frac{E}{\Gamma} - i\frac{\Gamma}{2} \left(\frac{U}{\pi\Gamma}\right)^2 \left(\frac{E}{\Gamma}\right)^2, \quad (32)$$

the exact results based on the Bethe ansatz method. [23, 24]

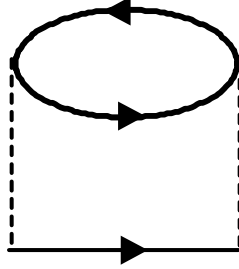


Figure 2. The diagram for the second-order self-energy. The solid line denotes the noninteracting Green's function and the dashed line denotes interaction.

The third-order terms corresponding to the diagram denoted in Fig. 3(a) are expressed by

$$\begin{aligned} \Sigma_{pp}^{r(3)}(E) &= U^3 \int_0^\infty dt_1 \int_{-\infty}^\infty dt_2 e^{iEt_1} \left[\begin{array}{l} g^<(-t_1)g^>(t_1-t_2)g^>(t_1-t_2) \\ -g^>(-t_1)g^<(t_1-t_2)g^<(t_1-t_2) \end{array} \right] \\ &\times \left[g^\pm(t_2)g^>(t_2) + g^<(t_2)g^\pm(t_2) \right], \end{aligned} \quad (33)$$

$$\begin{aligned} \Sigma_{pp}^{a(3)}(E) &= U^3 \int_{-\infty}^0 dt_1 \int_{-\infty}^\infty dt_2 e^{iEt_1} \left[\begin{array}{l} g^>(-t_1)g^<(t_1-t_2)g^<(t_1-t_2) \\ -g^<(-t_1)g^>(t_1-t_2)g^>(t_1-t_2) \end{array} \right] \\ &\times \left[g^\pm(t_2)g^>(t_2) + g^<(t_2)g^\pm(t_2) \right]. \end{aligned} \quad (34)$$

Figure 3(b) illustrates the diagram for the following terms:

$$\begin{aligned} \Sigma_{ph}^{r(3)}(E) &= U^3 \int_0^\infty dt_1 \int_{-\infty}^\infty dt_2 e^{iEt_1} \left[\begin{array}{l} g^>(t_1)g^>(t_1-t_2)g^<(t_2-t_1) \\ -g^<(t_1)g^<(t_1-t_2)g^>(t_2-t_1) \end{array} \right] \\ &\times \left[g^\pm(t_2)g^<(-t_2) + g^<(t_2)g^\pm(-t_2) \right], \end{aligned} \quad (35)$$

$$\begin{aligned} \Sigma_{ph}^{a(3)}(E) &= U^3 \int_{-\infty}^0 dt_1 \int_{-\infty}^\infty dt_2 e^{iEt_1} \left[\begin{array}{l} g^<(t_1)g^<(t_1-t_2)g^>(t_2-t_1) \\ -g^>(t_1)g^>(t_1-t_2)g^<(t_2-t_1) \end{array} \right] \\ &\times \left[g^\pm(t_2)g^<(-t_2) + g^<(t_2)g^\pm(-t_2) \right]. \end{aligned} \quad (36)$$

Equations (33)-(36) for equilibrium agree exactly with those derived from the Matsubara imaginary-time perturbative expansion for equilibrium and analytical continuity by Zlatić *et al.* [25] As mentioned later, it is numerically confirmed that the third-order contribution vanishes for the symmetric Anderson model; this is in good agreement with both the results brought from the Yamada-Yosida theory [14, 24, 26] and those obtained on the basis of the Bethe ansatz method. [23] If the step functions in Eqs. (17) and (18) is missing, then the expressions for the third-order cannot agree with those formulated by Zlatić *et al.* and do not cancel for electron-hole symmetry. As the consequence, it gives confirmation to the validity of the improvement expressed by Eqs. (17) and (18) and to Eq. (1) working as the Dyson's equation.

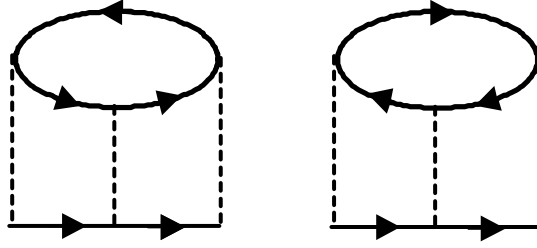


Figure 3. The two diagrams for the third-order self-energy. Left:(a) and Right:(b)

Furthermore, the fourth-order contribution to the self-energy is formulated. (See Appendix.) The twelve terms for the proper fourth-order self-energy can be divided into four groups, each of which comprises three terms. The four groups correspond to the diagrams denoted in Figs. 4 (a)-(c), Figs. 4 (d)-(f), Figs. 4 (g)-(i), and Figs. 4 (j)-(l), respectively. For symmetric Anderson model at equilibrium, the asymptotic behavior at low energy is approximately in agreement with those based on the Bethe ansatz method [23]:

$$\Sigma^{r(4)}(E) \simeq -\Gamma \left(105 - \frac{45\pi^2}{4} + \frac{\pi^4}{16} \right) \left(\frac{U}{\pi\Gamma} \right)^4 \frac{E}{\Gamma} - i \frac{\Gamma}{2} (30 - 3\pi^2) \left(\frac{U}{\pi\Gamma} \right)^4 \left(\frac{E}{\Gamma} \right)^2. \quad (37)$$

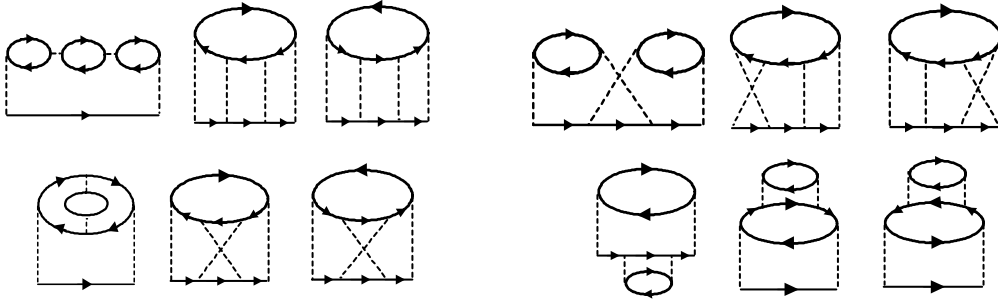


Figure 4. The twelve terms for the proper fourth-order self-energy divided into four groups: (a)-(c), (d)-(f), (g)-(i), and (j)-(l).

4. Numerical Results and Discussion

4.1. Self-Energy

The third-order terms, Eqs. (33)-(36) cancel under electron-hole symmetry not only at equilibrium but also at nonequilibrium: $\Sigma_{ph}^{r(3)}(E) = -\Sigma_{pp}^{r(3)}(E)$ and $\Sigma_{ph}^{a(3)}(E) = -\Sigma_{pp}^{a(3)}(E)$. As a consequence, the third-order contribution to self-energy vanishes in the symmetric case. In this connection, the results of Refs. [14, 24, 26] based on the Yamada-Yosida theory show that all odd-order contributions except the Hartree term vanish for equilibrium in the symmetric single-impurity Anderson model; probably, it is just the same with nonequilibrium state. On the other hand, the third-order terms contribute to the asymmetric system where electron-hole symmetry breaks and furthermore, the third-order terms for spin-up and for spin-down contribute respectively when the

spin degeneracy is lifted for example, by magnetic field. For the fourth-order contribution, three terms which constitute each of four groups contribute equivalently under electron-hole symmetry. Moreover, to the asymmetric system, the terms brought by the diagrams of Figs. 4(a) and 4(b) contribute equivalently and the terms by the diagrams of Figs. 4(j) and 4(k) make equivalent contribution, and the rest, the eight terms contribute respectively. Further, the twenty-four terms for spin-up and spin-down take effect severally in the presence of magnetic field.

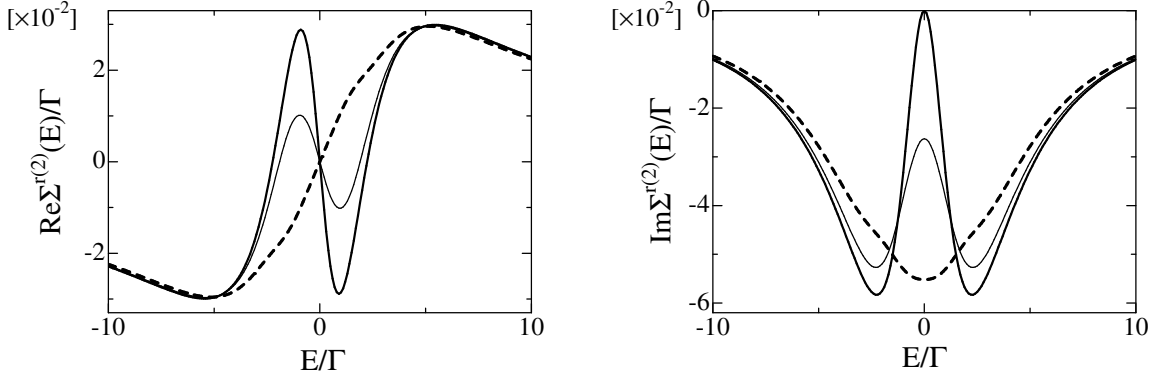


Figure 5. The second-order self-energy for the symmetric Anderson model at $U/\Gamma = 1.0$ and zero temperature. (a) The real part and (b) the imaginary part at equilibrium (solid line), $eV/\Gamma = 1.0$ (thin solid line), and $eV/\Gamma = 2.0$ (dashed line).

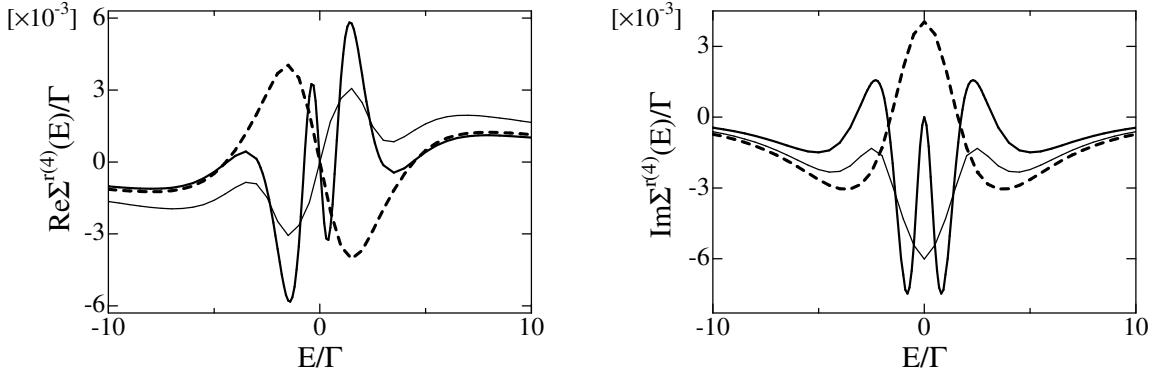


Figure 6. The fourth-order self-energy for the symmetric Anderson model at $U/\Gamma = 1.0$ and zero temperature. (a) The real part and (b) the imaginary part at equilibrium (solid line), $eV/\Gamma = 1.0$ (thin solid line), and $eV/\Gamma = 2.0$ (dashed line). The fourth-order contribution for equilibrium has the same but narrow curves at low energy with those of the second-order contribution.

The second-order and the fourth-order contributions to self-energy for zero temperature symmetric Anderson model are shown in Figs. 5(a) and 5(b) and in Figs. 6(a) and 6(b), respectively. Equation (32) represents the curves around $E = 0$ denoted by solid line in Figs. 5(a) and 5(b), respectively, and Equation (37) represents approximately those shown in Figs. 6(a) and 6(b), respectively. The curves of the second-order self-energy shown in Figs. 5(a) and 5(b) are identical with those of expressions derived by Hershfield *et al.* [15]. In comparison of Figs. 6(a) and 6(b) with Figs. 5(a) and 5(b), it is found that the fourth-order contribution for equilibrium has the same but narrow curves at low energy with those of the second-order contribution. In addition, the broad curves are attached at high energy for the fourth-order self-energy. (The higher-order contribution is, the more the curves of the contribution must oscillate as a function of energy.)

When the voltage, eV/Γ exceeds ~ 2.0 , the behavior of curves of self-energy changes distinctly and comes to present striking contrasts to that for the second-order contribution. Especially, the curve for the imaginary part of the fourth-order contribution rises up with maximum at $E = 0$. On the other hand, for the second-order contribution, a valley appears with minimum at energy of zero—it is quite the contrary. Moreover, from these results, it is expected that the sixth-order contribution to imaginary part of self-energy has minimum at $E = 0$. Because of these, the perturbative expansion is hard to converge for $eV/\Gamma > \sim 2.0$, as mentioned later.

Besides, the current conservation is mentioned. In Ref. [15], it is shown that the continuity of current entering and leaving the impurity stands exactly at any strength of U within the approximation up to the second-order for the symmetric single-impurity Anderson model. In comparison of Figs. 6(a) and 6(b) with Figs. 5(a) and 5(b), it is found that curves of fourth-order self-energy have the symmetry similar to those of the second-order. From this, it is anticipated that the current conservation are satisfied perfectly with approximation up to the fourth-order in the single-impurity system where electron-hole symmetry holds. The continuity of current can be maintained perfectly in single-impurity system as far as electron-hole symmetry stands. On the other hand, current comes to fail to be conserved with increasing U in asymmetric single-impurity case and in two-impurity case.

4.2. Spectral Function

The spectral function with the second-order self-energy is generally known. It is plotted for $U/\Gamma = 10.0$ and zero temperature in Fig. 7. For equilibrium, the Kondo peak at energy of zero is very sharp and the two-side broad peaks appear at $E \simeq \pm U/2$. The curve for $eV = 0$ is identical with that shown in Ref. [24]. As eV becomes higher than the Kondo temperature, $k_B T_K$ [27], the Kondo peak becomes lower and finally vanishes, while the two-side broad peaks rise at $E \simeq \pm U/2$. [15]

Figure 8 shows the spectral function with the self-energy up to the fourth-order for equilibrium and zero temperature. With strengthening U , two-side narrow peaks come to occur in the vicinity of $E = \pm U/2$ in addition to the Kondo peak. At U large enough, the Kondo peak becomes very acute and two-side narrow peaks rise higher and sharpen; the energy levels for the atomic limit are produced distinctly. The fourth-order self-energy has the same but narrow curves as functions of energy with those of the second-order and those curves make the peaks at $E = \pm U/2$.

For the present approximation up to the fourth-order, the Kondo peak at $E = 0$ reaches the unitarity limit and the charge, $\langle n \rangle$ corresponds to $1/2$, that is, the Friedel sum rule is correctly satisfied: [28]

$$\rho(E_f) = \sin^2(\pi \langle n \rangle) / \pi \Gamma, \quad (38)$$

where $\rho(E_f)$ is the local density of states at the Fermi energy. Here, the discussions should be made on the ranges of U in which the present approximation up to the fourth-order stands. From the results, it is found that the approximation within the fourth-order holds up to $U/\Gamma \sim 5.0$ and is beyond the validity for $U/\Gamma > \sim 6.0$. In addition, the curve for imaginary part of the fourth-order contribution is positive partly, as shown in Fig. 6(b) and as a consequence, the curve of the spectral function becomes negative partly for too large U . In such a case, the present approximation is out of validity and the higher-order terms are required.

Next, the results for nonequilibrium and zero temperature are shown. The expression for the Friedel sum rule, Eq. (38) does not stand for nonequilibrium, since the charge cannot be expressed with respect to the local density of states. However, the Kondo peak reaches the unitarity limit and $\langle n \rangle = 1/2$ in the symmetric and noninteracting case. The spectral functions with the self-energy up to the fourth-order are plotted for $eV/\Gamma = 0.5$ and $eV/\Gamma = 1.0$ in Figs. 9, respectively. When U is strengthened and eV exceeds $k_B T_K$ (approximately, $k_B T_K/\Gamma \sim 0.5$ for $U/\Gamma = 3.5$ and $k_B T_K/\Gamma \sim 0.3$ for $U/\Gamma = 5.0$), the Kondo peak for $eV/\Gamma = 0.5$ falls in and instead, the two-side narrow peaks remain to sharpen in the vicinity of $E = \pm U/2$. For $eV/\Gamma = 1.0$, the Kondo peak becomes broad and disappears for U large enough. The two-side peaks is generated small in the vicinity of $E = \pm U/2$. The Kondo resonance is quite broken for bias voltage exceeding the

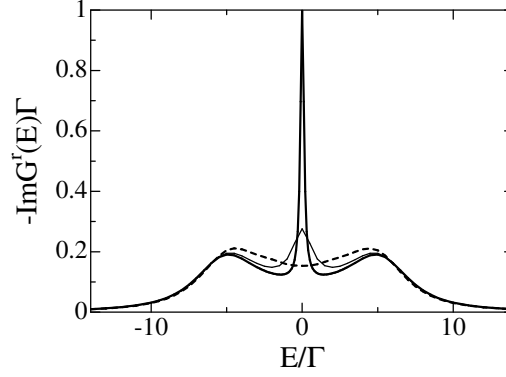


Figure 7. The spectral function with the second-order self-energy at $U/\Gamma = 10.0$ for the symmetric Anderson model at equilibrium (solid line), $eV/\Gamma = 1.0$ (thin solid line) and $eV/\Gamma = 2.0$ (dashed line).

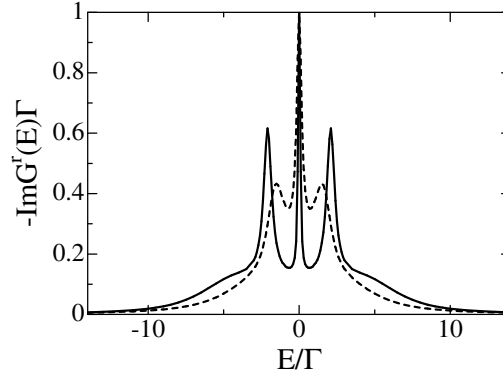


Figure 8. The spectral function with self-energy up to the fourth-order at equilibrium for the symmetric Anderson model at $U/\Gamma = 3.5$ (dashed line) and $U/\Gamma = 5.0$ (solid line).

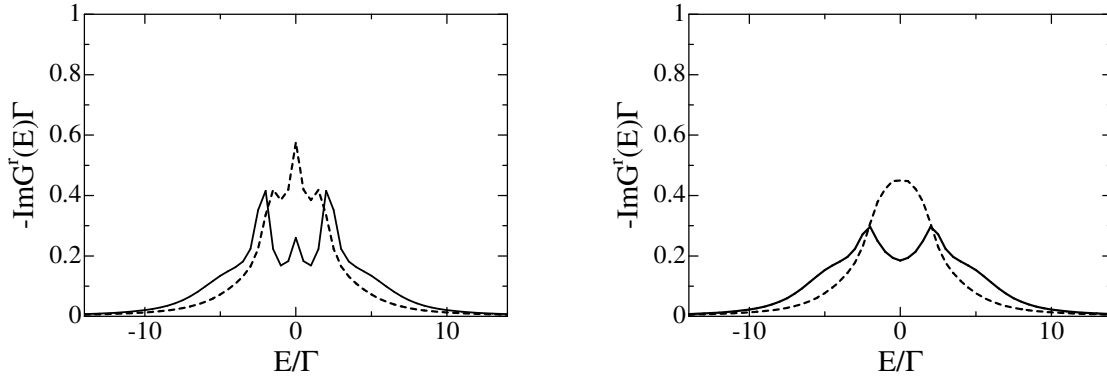


Figure 9. The spectral functions with self-energy up to the fourth-order at $eV/\Gamma = 0.5$ (Left) and $eV/\Gamma = 1.0$ (Right) for the symmetric Anderson model. $U/\Gamma = 3.5$ (dashed line) and $U/\Gamma = 5.0$ (solid line).

Kondo temperature; this accords with the experimental result that the Kondo effect is suppressed when source-drain bias voltage is comparable to or exceeds the Kondo temperature, $eV \geq k_B T_K$. [16, 17] For $eV/\Gamma > \sim 2.0$, the Kondo peak does not lower even when eV is much larger than $k_B T_K$. The perturbative expansion is hard to converge on account of the imaginary part of the self-energy for $eV/\Gamma > \sim 2.0$, as described before; thereby, the higher-order contribution to self-energy is probably needed for high voltage. In the present work, nonequilibrium state is represented as the superposition of the two leads and the effective Fermi distribution function, Eq. (29) is qualitatively similar to that for finite temperatures. From the analogy in the Fermi distribution function, it is inferred that there are nonequilibrium fluctuations similar to thermal fluctuations. Because of the effective Fermi distribution function, not only for the second-order but also for the fourth-order, the Kondo resonance is broken, qualitatively the same as for finite temperatures. The Kondo resonance splitting may not take place for finite bias voltage.

In conclusions, in the present work, the nonequilibrium perturbative formalism is reconsidered and the relationship for self-energy is generalized. As the consequence, it proves that some equations formally used do not stand and is indicated that the nonequilibrium (real-time) perturbative expansion can be related to the Matsubara imaginary-time perturbative expansion for equilibrium. In addition, it is shown that with this improvement, Equation (1) works as the Dyson's equation at least up to the fourth-order.

As the numerical results, the Kondo peak disappears as bias voltage exceeding the Kondo temperature. Because of the analogy of the effective Fermi distribution function for nonequilibrium with that for finite temperatures, the present result is qualitatively similar to that for finite temperatures. This characteristic is supported by the experiments.

Acknowledgements

The numerical calculations were executed at the Yukawa Institute Computer Facility. The multiple integrals were performed using the computer subroutine, *MQFSRD* of NUMPAC.

Appendix

The twelve terms for the fourth-order contribution can be divided into four groups, each of which is composed of three terms. The four groups are brought from diagrams denoted in Figs. 4 (a)-(c), Figs. 4 (d)-(f), Figs. 4 (g)-(i), and Figs. 4 (j)-(l), respectively. The terms for the diagrams illustrated in Figs. 4(a) and 4(b) are equivalent except for the spin indices and expressed by

$$\begin{aligned} \Sigma_{a,b}^{r(4)}(E) = & U^4 \int_0^\infty dt_1 \int_{-\infty}^\infty dt_2 \int_{-\infty}^\infty dt_3 e^{iEt_1} \\ & \times \left[\begin{array}{l} g^<(t_1)g^<(t_1-t_2-t_3)g^>(-t_1+t_2+t_3) \\ -g^>(t_1)g^>(t_1-t_2-t_3)g^<(-t_1+t_2+t_3) \end{array} \right] \\ & \times [g^\pm(t_2)g^<(-t_2) + g^<(t_2)g^\pm(-t_2)] \\ & \times [g^\pm(t_3)g^<(-t_3) + g^<(t_3)g^\pm(-t_3)], \end{aligned} \quad (39)$$

$$\begin{aligned} \Sigma_{a,b}^{a(4)}(E) = & U^4 \int_{-\infty}^0 dt_1 \int_{-\infty}^\infty dt_2 \int_{-\infty}^\infty dt_3 e^{iEt_1} \\ & \times \left[\begin{array}{l} g^>(t_1)g^>(t_1-t_2-t_3)g^<(-t_1+t_2+t_3) \\ -g^<(t_1)g^<(t_1-t_2-t_3)g^>(-t_1+t_2+t_3) \end{array} \right] \\ & \times [g^\pm(t_2)g^<(-t_2) + g^<(t_2)g^\pm(-t_2)] \\ & \times [g^\pm(t_3)g^<(-t_3) + g^<(t_3)g^\pm(-t_3)]. \end{aligned} \quad (40)$$

Additionally, Figure 4(c) shows the diagram for the following terms:

$$\begin{aligned}
\Sigma_c^{r(4)}(E) &= U^4 \int_0^\infty dt_1 \int_{-\infty}^\infty dt_2 \int_{-\infty}^\infty dt_3 e^{iEt_1} \\
&\times \left[g^>(-t_1)g^<(t_1-t_2-t_3)g^<(t_1-t_2-t_3) \right. \\
&\quad \left. - g^<(-t_1)g^>(t_1-t_2-t_3)g^>(t_1-t_2-t_3) \right] \\
&\times [g^\pm(t_2)g^>(t_2) + g^<(t_2)g^\pm(t_2)] \\
&\times [g^\pm(t_3)g^>(t_3) + g^<(t_3)g^\pm(t_3)], \tag{41}
\end{aligned}$$

$$\begin{aligned}
\Sigma_c^{a(4)}(E) &= U^4 \int_{-\infty}^0 dt_1 \int_{-\infty}^\infty dt_2 \int_{-\infty}^\infty dt_3 e^{iEt_1} \\
&\times \left[g^<(-t_1)g^>(t_1-t_2-t_3)g^>(t_1-t_2-t_3) \right. \\
&\quad \left. - g^>(-t_1)g^<(t_1-t_2-t_3)g^<(t_1-t_2-t_3) \right] \\
&\times [g^\pm(t_2)g^>(t_2) + g^<(t_2)g^\pm(t_2)] \\
&\times [g^\pm(t_3)g^>(t_3) + g^<(t_3)g^\pm(t_3)]. \tag{42}
\end{aligned}$$

Next, the terms brought from diagram in Fig. 4(d) are expressed by

$$\begin{aligned}
\Sigma_d^{r(4)}(E) &= U^4 \int_0^\infty dt_1 \int_{-\infty}^\infty dt_2 \int_{-\infty}^\infty dt_3 e^{iEt_1} \\
&\times \left[g^>(t_1-t_3)g^>(t_1-t_2)g^<(t_2-t_1) \right. \\
&\quad \left. - g^<(t_1-t_3)g^<(t_1-t_2)g^>(t_2-t_1) \right] \\
&\times g^\pm(t_2) \operatorname{sgn}(t_3) \left[g^>(-t_2+t_3)g^>(t_3)g^<(-t_3) \right. \\
&\quad \left. - g^<(-t_2+t_3)g^<(t_3)g^>(-t_3) \right], \tag{43}
\end{aligned}$$

$$\begin{aligned}
\Sigma_d^{a(4)}(E) &= U^4 \int_{-\infty}^0 dt_1 \int_{-\infty}^\infty dt_2 \int_{-\infty}^\infty dt_3 e^{iEt_1} \\
&\times \left[g^<(t_1-t_3)g^<(t_1-t_2)g^>(t_2-t_1) \right. \\
&\quad \left. - g^>(t_1-t_3)g^>(t_1-t_2)g^<(t_2-t_1) \right] \\
&\times g^\pm(t_2) \operatorname{sgn}(t_3) \left[g^>(-t_2+t_3)g^>(t_3)g^<(-t_3) \right. \\
&\quad \left. - g^<(-t_2+t_3)g^<(t_3)g^>(-t_3) \right]. \tag{44}
\end{aligned}$$

The terms for diagram in Fig. 4(e) are written by

$$\begin{aligned}
\Sigma_e^{r(4)}(E) &= U^4 \int_0^\infty dt_1 \int_{-\infty}^\infty dt_2 \int_{-\infty}^\infty dt_3 e^{iEt_1} \\
&\times \left[g^>(t_1-t_2)g^>(t_1-t_2)g^<(t_3-t_1) \right. \\
&\quad \left. - g^<(t_1-t_2)g^<(t_1-t_2)g^>(t_3-t_1) \right] \\
&\times g^\pm(t_2) \operatorname{sgn}(t_3) \left[g^>(t_2-t_3)g^>(-t_3)g^<(t_3) \right. \\
&\quad \left. - g^<(t_2-t_3)g^<(-t_3)g^>(t_3) \right], \tag{45}
\end{aligned}$$

$$\begin{aligned}
\Sigma_e^{a(4)}(E) &= U^4 \int_{-\infty}^0 dt_1 \int_{-\infty}^\infty dt_2 \int_{-\infty}^\infty dt_3 e^{iEt_1} \\
&\times \left[g^<(t_1-t_2)g^<(t_1-t_2)g^>(t_3-t_1) \right. \\
&\quad \left. - g^>(t_1-t_2)g^>(t_1-t_2)g^<(t_3-t_1) \right] \\
&\times g^\pm(t_2) \operatorname{sgn}(t_3) \left[g^>(t_2-t_3)g^>(-t_3)g^<(t_3) \right. \\
&\quad \left. - g^<(t_2-t_3)g^<(-t_3)g^>(t_3) \right]. \tag{46}
\end{aligned}$$

In addition, Figure 4(f) denotes the diagram for the following terms:

$$\begin{aligned}\Sigma_f^{r(4)}(E) &= U^4 \int_0^\infty dt_1 \int_{-\infty}^\infty dt_2 \int_{-\infty}^\infty dt_3 e^{iEt_1} \\ &\times \left[\begin{array}{l} g^>(t_1 - t_3)g^>(t_1 - t_2)g^<(t_2 - t_1) \\ -g^<(t_1 - t_3)g^<(t_1 - t_2)g^>(t_2 - t_1) \end{array} \right] \\ &\times g^\pm(-t_2) \text{sgn}(t_3) \left[\begin{array}{l} g^<(t_3)g^<(t_3)g^>(t_2 - t_3) \\ -g^>(t_3)g^>(t_3)g^<(t_2 - t_3) \end{array} \right],\end{aligned}\quad (47)$$

$$\begin{aligned}\Sigma_f^{a(4)}(E) &= U^4 \int_{-\infty}^0 dt_1 \int_{-\infty}^\infty dt_2 \int_{-\infty}^\infty dt_3 e^{iEt_1} \\ &\times \left[\begin{array}{l} g^<(t_1 - t_3)g^<(t_1 - t_2)g^>(t_2 - t_1) \\ -g^>(t_1 - t_3)g^>(t_1 - t_2)g^<(t_2 - t_1) \end{array} \right] \\ &\times g^\pm(-t_2) \text{sgn}(t_3) \left[\begin{array}{l} g^<(t_3)g^<(t_3)g^>(t_2 - t_3) \\ -g^>(t_3)g^>(t_3)g^<(t_2 - t_3) \end{array} \right].\end{aligned}\quad (48)$$

Next, the terms formulated from diagram illustrated in Fig. 4(g) are expressed by

$$\begin{aligned}\Sigma_g^{r(4)}(E) &= U^4 \int_0^\infty dt_1 \int_{-\infty}^\infty dt_2 \int_{-\infty}^\infty dt_3 e^{iEt_1} \\ &\times \left[\begin{array}{l} g^>(t_1)g^>(t_1 - t_2 - t_3)g^<(t_2 - t_1) \\ -g^<(t_1)g^<(t_1 - t_2 - t_3)g^>(t_2 - t_1) \end{array} \right] \\ &\times g^\pm(-t_2) \text{sgn}(t_3) \left[\begin{array}{l} g^>(t_2 + t_3)g^>(t_3)g^<(-t_3) \\ -g^<(t_2 + t_3)g^<(t_3)g^>(-t_3) \end{array} \right],\end{aligned}\quad (49)$$

$$\begin{aligned}\Sigma_g^{a(4)}(E) &= U^4 \int_{-\infty}^0 dt_1 \int_{-\infty}^\infty dt_2 \int_{-\infty}^\infty dt_3 e^{iEt_1} \\ &\times \left[\begin{array}{l} g^<(t_1)g^<(t_1 - t_2 - t_3)g^>(t_2 - t_1) \\ -g^>(t_1)g^>(t_1 - t_2 - t_3)g^<(t_2 - t_1) \end{array} \right] \\ &\times g^\pm(-t_2) \text{sgn}(t_3) \left[\begin{array}{l} g^>(t_2 + t_3)g^>(t_3)g^<(-t_3) \\ -g^<(t_2 + t_3)g^<(t_3)g^>(-t_3) \end{array} \right].\end{aligned}\quad (50)$$

Figure 4(h) illustrates the diagram for the following terms:

$$\begin{aligned}\Sigma_h^{r(4)}(E) &= U^4 \int_0^\infty dt_1 \int_{-\infty}^\infty dt_2 \int_{-\infty}^\infty dt_3 e^{iEt_1} \\ &\times \left[\begin{array}{l} g^<(t_1)g^<(t_1 - t_2 - t_3)g^>(t_2 - t_1) \\ -g^>(t_1)g^>(t_1 - t_2 - t_3)g^<(t_2 - t_1) \end{array} \right] \\ &\times g^\pm(t_2) \text{sgn}(t_3) \left[\begin{array}{l} g^>(t_3)g^>(t_3)g^<(-t_2 - t_3) \\ -g^<(t_3)g^<(t_3)g^>(-t_2 - t_3) \end{array} \right],\end{aligned}\quad (51)$$

$$\begin{aligned}\Sigma_h^{a(4)}(E) &= U^4 \int_{-\infty}^0 dt_1 \int_{-\infty}^\infty dt_2 \int_{-\infty}^\infty dt_3 e^{iEt_1} \\ &\times \left[\begin{array}{l} g^>(t_1)g^>(t_1 - t_2 - t_3)g^<(t_2 - t_1) \\ -g^<(t_1)g^<(t_1 - t_2 - t_3)g^>(t_2 - t_1) \end{array} \right] \\ &\times g^\pm(t_2) \text{sgn}(t_3) \left[\begin{array}{l} g^>(t_3)g^>(t_3)g^<(-t_2 - t_3) \\ -g^<(t_3)g^<(t_3)g^>(-t_2 - t_3) \end{array} \right].\end{aligned}\quad (52)$$

Besides, the terms formulated from the diagram in Fig. 4(i) are written by

$$\begin{aligned}\Sigma_i^{r(4)}(E) &= U^4 \int_0^\infty dt_1 \int_{-\infty}^\infty dt_2 \int_{-\infty}^\infty dt_3 e^{iEt_1} \\ &\times \left[\begin{array}{c} g^>(-t_1)g^<(t_1-t_2-t_3)g^<(t_1-t_2) \\ -g^<(-t_1)g^>(t_1-t_2-t_3)g^>(t_1-t_2) \end{array} \right] \\ &\times g^\pm(t_2) \operatorname{sgn}(t_3) \left[\begin{array}{c} g^>(t_2+t_3)g^>(t_3)g^<(-t_3) \\ -g^<(t_2+t_3)g^<(t_3)g^>(-t_3) \end{array} \right],\end{aligned}\quad (53)$$

$$\begin{aligned}\Sigma_i^{a(4)}(E) &= U^4 \int_{-\infty}^0 dt_1 \int_{-\infty}^\infty dt_2 \int_{-\infty}^\infty dt_3 e^{iEt_1} \\ &\times \left[\begin{array}{c} g^<(-t_1)g^>(t_1-t_2-t_3)g^>(t_1-t_2) \\ -g^>(-t_1)g^<(t_1-t_2-t_3)g^<(t_1-t_2) \end{array} \right] \\ &\times g^\pm(t_2) \operatorname{sgn}(t_3) \left[\begin{array}{c} g^>(t_2+t_3)g^>(t_3)g^<(-t_3) \\ -g^<(t_2+t_3)g^<(t_3)g^>(-t_3) \end{array} \right].\end{aligned}\quad (54)$$

Next, the terms for diagrams denoted in Figs. 4 (j) and 4(k) are equivalent except for the spin indices and written by

$$\begin{aligned}\Sigma_{j,k}^{r(4)}(E) &= U^4 \int_0^\infty dt_1 \int_{-\infty}^\infty dt_2 \int_{-\infty}^\infty dt_3 e^{iEt_1} \\ &\times \left[\begin{array}{c} g^>(t_1)g^<(-t_1)g^>(t_1-t_2-t_3) \\ -g^<(t_1)g^>(-t_1)g^<(t_1-t_2-t_3) \end{array} \right] \\ &\times g^\pm(t_2) \left[\begin{array}{c} g^\pm(t_3)g^>(t_3)g^<(-t_3) \\ +g^<(t_3)g^\pm(t_3)g^>(-t_3) \\ +g^<(t_3)g^>(t_3)g^\pm(-t_3) \end{array} \right],\end{aligned}\quad (55)$$

$$\begin{aligned}\Sigma_{j,k}^{a(4)}(E) &= U^4 \int_{-\infty}^0 dt_1 \int_{-\infty}^\infty dt_2 \int_{-\infty}^\infty dt_3 e^{iEt_1} \\ &\times \left[\begin{array}{c} g^<(t_1)g^>(-t_1)g^<(t_1-t_2-t_3) \\ -g^>(t_1)g^<(-t_1)g^>(t_1-t_2-t_3) \end{array} \right] \\ &\times g^\pm(t_2) \left[\begin{array}{c} g^\pm(t_3)g^>(t_3)g^<(-t_3) \\ +g^<(t_3)g^\pm(t_3)g^>(-t_3) \\ +g^<(t_3)g^>(t_3)g^\pm(-t_3) \end{array} \right].\end{aligned}\quad (56)$$

In addition, the terms for diagram illustrated in Fig. 4(l) are expressed by

$$\begin{aligned}\Sigma_l^{r(4)}(E) &= U^4 \int_0^\infty dt_1 \int_{-\infty}^\infty dt_2 \int_{-\infty}^\infty dt_3 e^{iEt_1} \\ &\times \left[\begin{array}{c} g^>(t_1)g^>(t_1)g^<(-t_1+t_2+t_3) \\ -g^<(t_1)g^<(t_1)g^>(-t_1+t_2+t_3) \end{array} \right] \\ &\times g^\pm(-t_2) \left[\begin{array}{c} g^\pm(-t_3)g^>(-t_3)g^<(t_3) \\ +g^<(-t_3)g^\pm(-t_3)g^>(t_3) \\ +g^<(-t_3)g^>(-t_3)g^\pm(t_3) \end{array} \right],\end{aligned}\quad (57)$$

$$\begin{aligned}\Sigma_l^{a(4)}(E) &= U^4 \int_{-\infty}^0 dt_1 \int_{-\infty}^\infty dt_2 \int_{-\infty}^\infty dt_3 e^{iEt_1} \\ &\times \left[\begin{array}{c} g^<(t_1)g^<(t_1)g^>(-t_1+t_2+t_3) \\ -g^>(t_1)g^>(t_1)g^<(-t_1+t_2+t_3) \end{array} \right] \\ &\times g^\pm(-t_2) \left[\begin{array}{c} g^\pm(-t_3)g^>(-t_3)g^<(t_3) \\ +g^<(-t_3)g^\pm(-t_3)g^>(t_3) \\ +g^<(-t_3)g^>(-t_3)g^\pm(t_3) \end{array} \right].\end{aligned}\quad (58)$$

References

1. Schwinger J. , J. Math. Phys. (N. Y.) 1961, **2**, 407.
2. Keldysh L. V. , Sov. Phys. JETP, 1965, **20**, 1018.
3. Kondo J. , Prog. Theor. Phys., 1964, **32**, 37.
4. Nozières P. , J. Low Temp. Phys., 1974, **17**, 31.
5. Wilson K. G. , Rev. Mod. Phys., 1975, **47**, 773.
6. Anderson P. W. , J. Phys. C, 1970,**3**, 2436.
7. Nozières P. and Blandin A. , J. Physique, 1980,**41**, 193.
8. Affleck I. , J. Phys. Soc. Jpn., 2005, **74**, 56.
9. Ng T.-K. and Lee P. A. , Phys. Rev. Lett., 1988, **61**, 1768; Glazman L. I. and Raikh M. E. , JETP Lett., 1988, **47**, 452.
10. Goldhaber-Gordon D. , Shtrikman H. , Mahalu D. , Abusch-Magder D. , Meirav U. and Kastner M. A. , Nature, 1998, **391**, 156.
11. van der Wiel W. G. , De Franceschi S. , Fujisawa T. , Elzerman J. M. , Tarucha S. , and Kouwenhoven L. P. , Science, 2000,**289**, 2105.
12. Haldane F. D. M. , Phys. Rev. Lett, 1978, **40**, 416.
13. Cronenwett S. M. , Tjerk H., Oosterkamp T. H. and Kouwenhoven L. P. , Science, 1998, **281**, 540.
14. Yosida K. and Yamada K. , Prog. Theor. Phys. Suppl., 1970, **46**, 244.
15. Hershfield S. , Davies J. H. and Wilkins J. W. , Phys. Rev. B, 1992, **46**, 7046.
16. Nygard J. , Koehl W. F. , Mason N. , DiCarlo L. and Marcus C. M. , “Zero-field splitting of Kondo resonances in a carbon nanotube quantum dot ”, Preprint arXiv:cond-mat/0410467,2004.
17. De Franceschi S. , Hanson R. , van der Wiel W. G. , Elzerman J. M. , Wijkema J. J. , Fujisawa T. , Tarucha S. , and Kouwenhoven L. P., Phys. Rev. Lett, 2002, **89**, 156801.
18. Caroli C. , Combescot R. , Nozières P. and Saint-James D. , J. Phys. C, 1971, **4**, 916.
19. Lifshitz E. M. and Pitaevskii L. P. , *Physical Kinetics* (Pergamon Press, 1981).
20. Zagoskin A. , *Quantum Theory of Many-Body Systems* (Springer-Verlag, 1998).
21. Huang K. , *Quantum Field Theory* (John Wiley & Sons, Inc.,1998).
22. Oguri A. , J. Phys. Soc. Jpn., 2002, **71**, 2969.
23. Okiji A. , *Fermi Surface Effects* edited by Kondo J. and Yoshimori A. (Springer, 1988).
24. Yamada K. , Prog. Theor. Phys., 1975, **53** 970; Prog. Theor. Phys., 1976, **55**, 1345.
25. Zlatić V. , Horvatić B. , Dolićki B. , Grabowski S. , Entel P. , and Schotte K.-D. , Phys. Rev. B, 2000, **63**, 35104.
26. Horvatić B. and Zlatić V. , Phys. Stat. Sol. (b), 1980, **99**, 251.
27. Zlatić V. and Horvatić B. , Phys. Rev. B, 1983,**28**, 6904.
28. Hewson A. C. , *The Kondo Problem to Heavy Fermions* (Cambridge University Press, Cambridge, 1993).